Instruments and Experimental Techniques, Vol. 43, No. 5, 2000, pp. 664–670. Translated from Pribory i Tekhnika Eksperimenta, No. 5, 2000, pp. 90–96.
Original Russian Text Copyright © 2000 by Touryanskii, Pirshin.

US28

GENERAL EXPERIMENTAL TECHNIQUES

A Method for the Formation of Ultrathin X-ray Beams

A. G. Touryanskii and I. V. Pirshin

Lebedev Physics Institute, Russian Academy of Science, Leninskii pr. 53, Moscow, 117924 Russia

Received March 3, 2000

Abstract—It is demonstrated that ultrathin beams with an effective cross section $h \leq 100$ nm and an angular divergence $\Delta\varphi \leq 2'$ below the diffraction limit can be obtained. This is achieved by irradiating the edge of an optically polished face by an X-ray beam with a wavelength of ~0.1 nm at a grazing angle close to the critical angle of total external reflection and subsequent transmission of the refracted beam through an adjacent side face. Under conditions ensuring effective h values of 81 and 96 nm, the values of $\Delta\varphi$ observed experimentally for GaAs and Si samples at wavelengths of 0.154 and 0.139 nm are much smaller than the diffraction limit calculated according to the theory of prism spectrometers. This allows for the formation of an X-ray probe that can be used for local analysis, for example, and layer-by-layer investigations of thin film structures.

INTRODUCTION

At present, X-ray methods in diffractometry, reflectometry, and small-angle scattering are widely used in studies of micro- and nanostructures on surfaces or in the bulks of various objects. In these cases, probe radiation with a wavelength $\lambda \sim 1$ Å is most frequently used, from which stringently collimated ribbon beams with an effective cross-sectional width $h = 30$–100 μm are formed. It is obvious that a selective analysis of thin layers is impossible with such beam dimensions. Investigation of the distributions of parameters along the sample's surface is also impeded, because measurements are usually performed at angles of beam inclination $\theta < \pi/2$, and the area of the irradiated zone thus increases proportionally to $1/\sin\theta$.

It is fairly easy to manufacture thin (e.g., with a width of ~100 nm) slit holes. However, the angular divergence $\Delta\varphi$ of the X-ray beam transmitted through such a hole is determined by the diffraction limit λ/h [1, 2]. This is confirmed by the results obtained in an X-ray waveguide formed by a Ni–C–Ni film structure [3]. In addition, the relative contribution of the small-angle scattering by the wall roughness of the slit channel to the beam side wings increases approximately proportionally to h^{-1} (all other conditions being equal), since the transmitted radiation intensity falls and the scattered one remains virtually unaltered. We should also note that a slit design with a hole in the absorbing shield prevents recording of the radiation, which is reflected or scattered at large angles, at short distances from the sample.

The problem of beam divergence also arises when using slit diaphragms with optically smooth surfaces of the interior channel and a system of microcapillaries [4, 5], because specular reflections with a reflectivity of ~1 occur at the interior surface at grazing angles smaller than the critical angle of total external reflection (TER) θ_c of the diaphragm material. For example, in operation with the CuK_α (8.05 keV) and FeK_α (6.40 keV) characteristic lines, the θ_c values range from 0.2° to 0.6° for most inorganic materials. Since $\Delta\varphi \sim \theta_c$, precise structural measurements become impossible at these values of the angular divergence, and the cross section of the beam emerging from the channel rapidly increases.

This work shows that slightly diverging ribbon beams with ultimately small cross-sectional widths can be obtained with the help of refraction at the edge of an optically polished face. In this case, the grazing angle of the primary beam, its divergence, and the real and imaginary parts of the refractive-index decrement are significant quantities.

Let us apply the approximation of geometric optics to the propagation of a parallel X-ray beam in a medium with a refractive index $n_1 = 1 - \delta_1 - i\beta_1$ passing through a corner of a prism with mutually perpendicular plane faces and a refractive index $n_2 = 1 - \delta_2 - i\beta_2$ (Fig. 1). Here, δ_1, δ_2 and $i\beta_1$, $i\beta_2$ are, respectively, the real and imaginary parts of the decrement of the refractive index. Let the axis z be normal to the first interface, and the axis x be parallel to it and lie in the incidence plane. We assume for definitiveness that the radiation is monochromatic with $\lambda \sim 0.1$ nm, and that the angle of incidence φ on the first interface is close to $\pi/2$. Under these conditions, we may analyze only the refraction at the first interface, because the values of the reflection coefficient and the relative variation of the refraction angle are negligibly small at the intersection of the second boundary. Changing from the angles of incidence to the grazing angles according to the formula $\theta = \pi/2 - \varphi$, the sine law [1, 2] can be transformed into the form

$$\frac{1 - \delta_1 - i\beta_1}{1 - \delta_2 - i\beta_2} = \frac{\sqrt{1 - \sin^2\theta_2}}{\sqrt{1 - \sin^2\theta_1}}, \quad (1)$$

0020-4412/00/4305-0664$25.00 © 2000 MAIK "Nauka /Interperiodica"

where θ_1 and θ_2 are the grazing angles of the incident and refracted radiation in the medium and prism material, respectively.

The magnitude of the refractive-index decrement $|\delta + i\beta|$ at the aforementioned wavelength is $<10^{-4}$ for all solids, and $\beta/\delta \ll 1$. This allows us to derive the following expression for the grazing angle of the refracted beam (for small angles $\theta_1 \ll \pi/2$):

$$\theta_2 \cong \sqrt{\theta_1^2 - 2(\delta_2 - \delta_1)}. \quad (2)$$

Assuming the medium to be vacuum (air) with $n_1 = 1$, we have

$$\theta_2 \cong \sqrt{\theta_1^2 - 2\delta_2}. \quad (3)$$

As shown in Fig. 1, upon passage through the first boundary, the contraction coefficient C_s of the beam cross section is

$$C_s = h_1/h_2 = \theta_1/\theta_2 = \theta_1/\sqrt{\theta_1^2 - 2(\delta_2 - \delta_1)}. \quad (4)$$

By differentiating expression (2) with respect to θ_1, we obtain the following dependence of the angular contraction coefficient on θ_1 for a beam with an angular divergence $\Delta\theta$ (θ_1 is the grazing angle of the central ray):

$$C_a = \Delta\theta_1/\Delta\theta_2 = \frac{\sqrt{\theta_1^2 - 2(\delta_2 - \delta_1)}}{\theta_1} = C_s^{-1}. \quad (5)$$

If $\theta_1 > \theta_c = (2\delta)^{-1/2}$, under the conditions mentioned above, the wave vector of the refracted wave is directed at a small angle to the surface, and the amplitude of the wave propagating into the sample decreases according to the law $\exp[-2\pi\beta z/(\lambda\theta_2)]$. Consequently, the planes of constant amplitudes are parallel to the interface, and the angle between the constant-phase plane and the interface is $\pi/2 - \theta_2$. The lines of intersection of the planes mentioned above with the plane of incidence are denoted as P_A and P_F in Fig. 1.

Figure 2 shows the dependence of the depth z_e, at which the intensity of the refracted radiation decreases by a factor e, on the grazing angle θ_1 for the CuK_α monochromatic radiation (0.154 nm) and several materials. The parameter z_e is actually a measure of the effective width of the beam emerging through the side face of the prism.

As expressions (3)–(5) show, in order to achieve maximum contraction of the X-ray beam cross section, it is necessary that, first, the radiation enters a less dense medium (i.e., Ren_1 > Ren_2), and, second, that the grazing angle θ_1 be close to θ_c. This can be achieved experimentally by irradiating the edge of an optically polished sample, the side surface of which was formed by splitting along a cleavage plane. In this case, the divergence of the primary beam must be minimal,

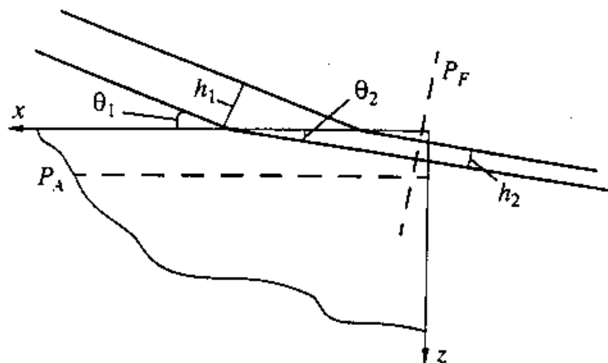

Fig. 1. Geometry of the trajectories of X-rays refracted at the edge of a rectangular prism.

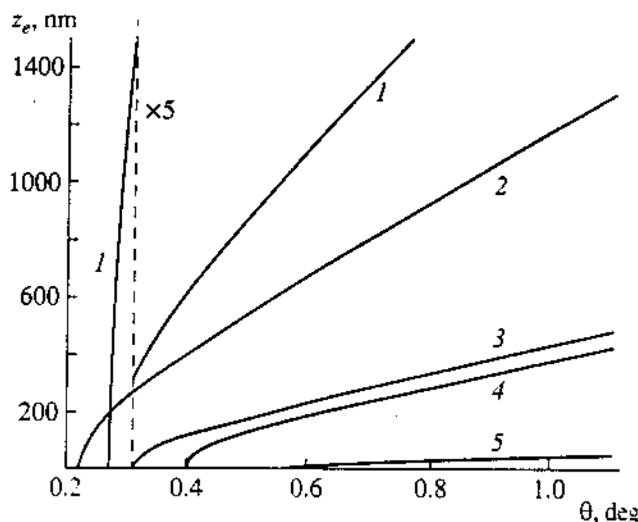

Fig. 2. Values of z_e in various refracted materials as a function of grazing angle θ_1 for CuK_α radiation: (*1–3*) diamond, Si, and GaAs single crystals, respectively; (*4, 5*) Ni (ρ = 8.9 g/cm^3) and W (ρ = 19.35 g/cm^3) polycrystals, respectively.

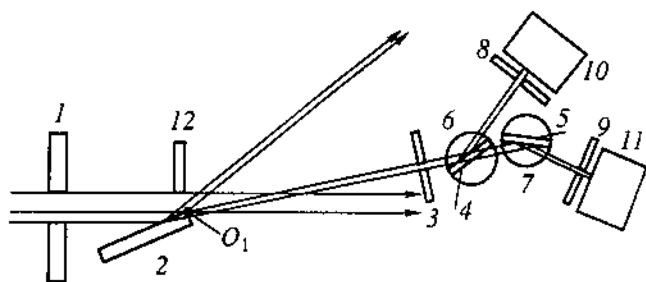

Fig. 3. Schematic diagram of the system for refraction measurements at two characteristic spectrum lines: (*1*) collimating slit; (*2*) sample; (*3*) entrance slit; (*4, 5*) monochromators; (*6, 7*) holders of the monochromators; (*8, 9*) slit diaphragms; (*10, 11*) detectors; and (*12*) absorbing shield.

because, in accordance with Eq. (5), the angular divergence of the refracted beam increases. Refraction was observed earlier in [6, 7] under such conditions as a spurious or subsidiary effect.

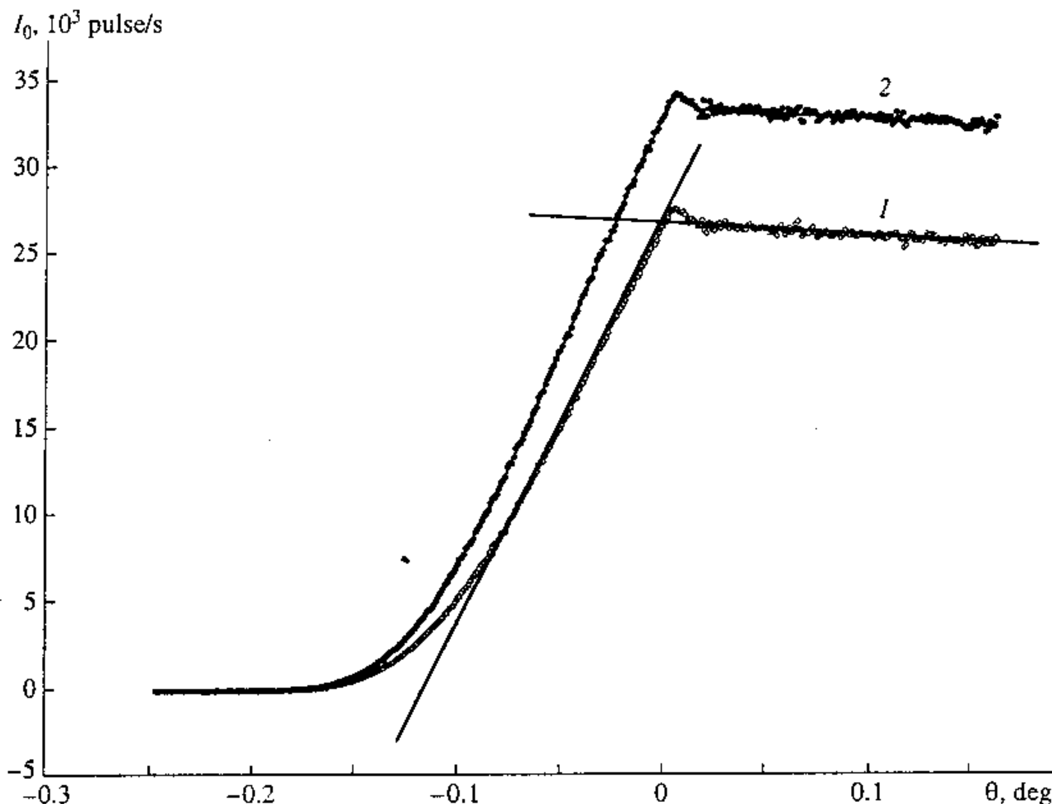

Fig. 4. Intensity of radiation passing through the gap between the sample and shield versus the angle of sample rotation θ: (*1*) CuK_α and (*2*) CuK_β.

MEASUREMENT SYSTEM

The above considerations were tested experimentally by using a two-wave reflectometer based on semitransparent monochromators manufactured from pyrolythic graphite (Fig. 3) [8]. The sample 2 was irradiated by a beam of polychromatic radiation of a copper-anode X-ray tube. In the measurement plane, the angular divergence of the beam incident on the area, which is adjacent to the O_1-axis, was 24″. The distance between the O_1-axis and the entrance slit was 225 mm. Monochromators *4* and *5* were adjusted to the CuK_α and CuK_β characteristic lines. The diffracted radiation was detected by independent scintillation detectors *10* and *11*. The entrance slit *3*, monochromators *4* and *5*, and detectors *10* and *11* were located on a rotating support with the rotational axis coinciding with that of the sample. This allowed us to measure simultaneously the intensity diagrams for both characteristic lines in a single angular scanning cycle. In order to estimate the angular resolution and the half-width of the refracted beams, the intensity distribution in the plane normal to the primary beam was recorded on a film. Rectangular plates of optically polished Si, GaAs, and natural diamond crystals 350–400 μm thick were used as refracting elements (refractors).

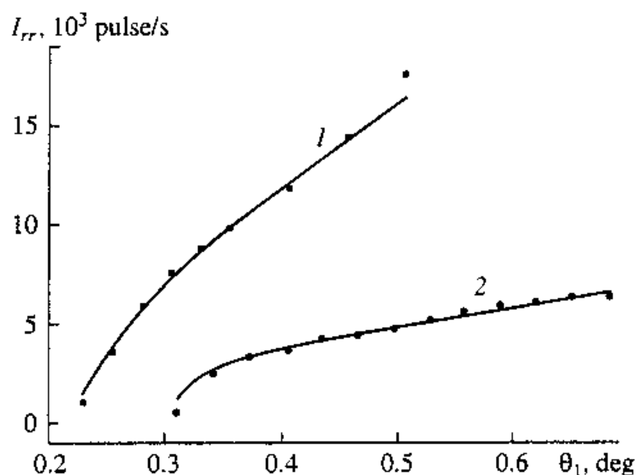

Fig. 5. Calculated (solid line) and experimental (dots) intensities of the refracted radiation versus the grazing angle θ_1 for (*1*) Si and (*2*) GaAs samples.

EXPERIMENTAL RESULTS

Direct measurements of the density distribution of an X-ray flux along the *z*-axis just behind the sample's side face, through which the refracted radiation leaves the sample, are impossible, because, at present, there

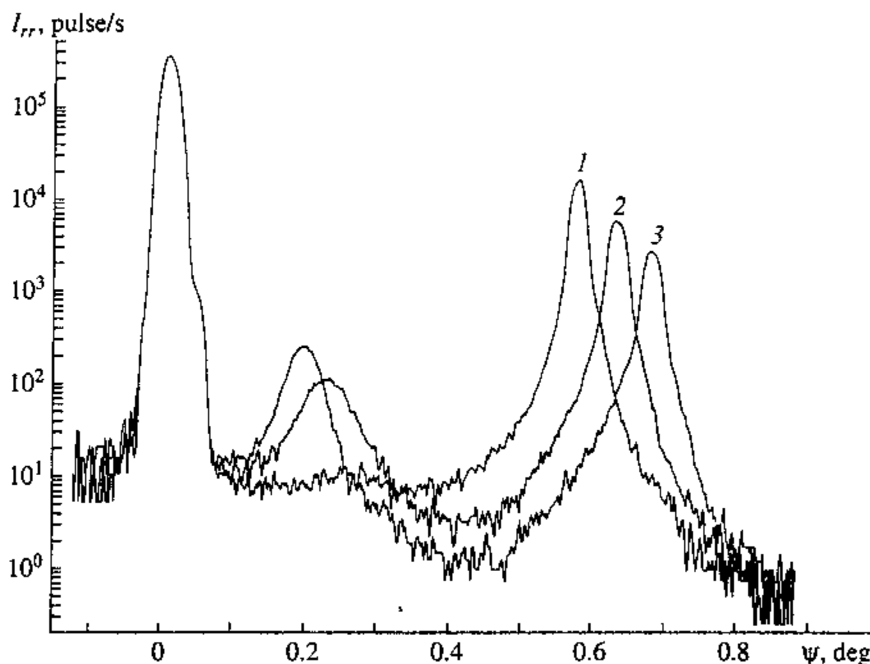

Fig. 6. Angular diagrams of the CuK_α line intensity for refraction at the edge of a GaAs plate for various grazing angles θ_1: (*1*) 0.285° [$\theta_1 > \theta_c$(CuK_β), $\theta_1 < \theta_c$(CuK_α)]; (*2*) 0.324° [$\theta_1 > \theta_c$(CuK_α) > θ_c(CuK_β)]; (*3*) 0.342°.

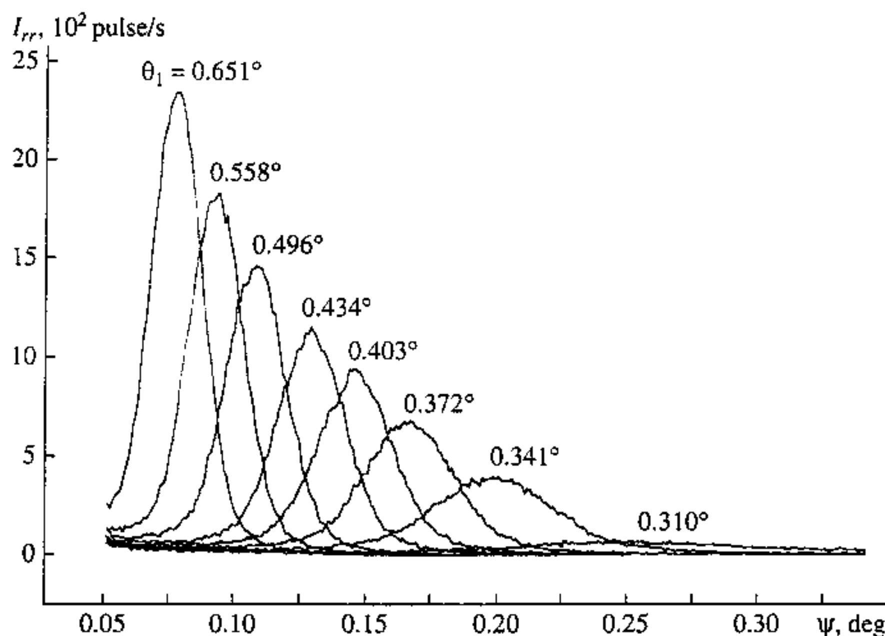

Fig. 7. Refractograms of a GaAs plate at the CuK_α line for various grazing angles of the primary beam.

exists no one- or two-coordinate X-ray detectors with a spatial resolution of ~10 nm. Therefore, we compared the calculated and experimental integral intensities of the refracted radiation. When determining the exact value of the X-ray flux density, the sample was set so that the sample's rotational axis O_1 was close to the side face through which the refracted radiation emerges. The sample's size in the measurement plane was 11 mm, and the ratio of the distances from the near and far edges of the surface to the O_1-axis was 3 : 100. The entrance slit with a width of 0.25 mm was set up on the path of the primary beam passing through the gap between the sample and absorbing shield. The forward radiation intensity I_0 was recorded as a function of the angle of rotation of the sample θ (Fig. 4). For an angular scanning step of 0.001°, the near and far edges of the sample

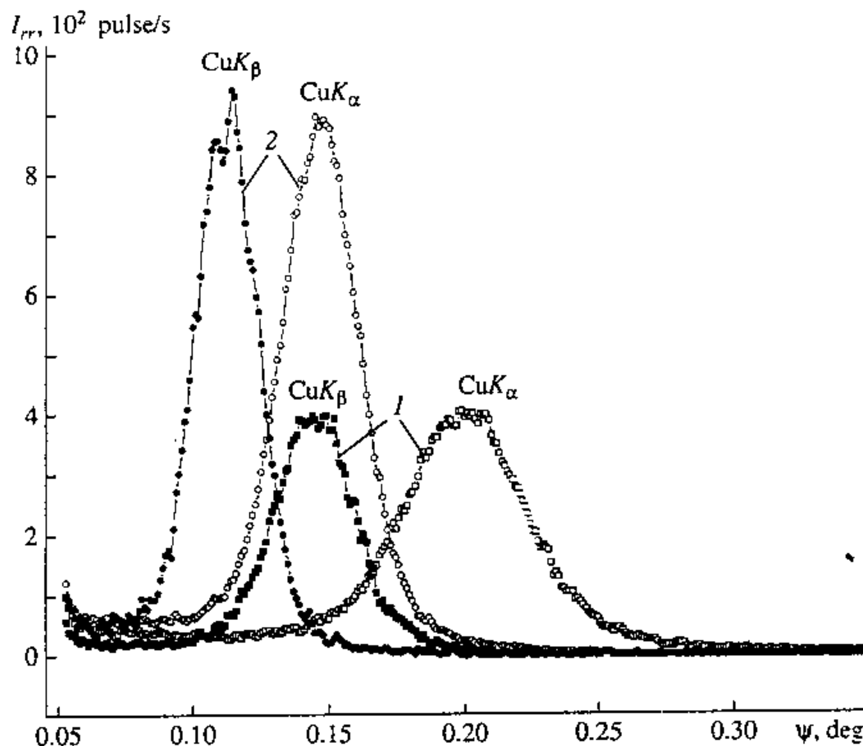

Fig. 8. Angular diagrams of the CuK_α and CuK_β line intensities for refraction at the edge of a GaAs plate for two grazing angles: θ_1 = (*1*) $1.1\theta_c$ and (*2*) $1.3\theta_c$.

must be displaced by 5.6 and 187 nm. This is confirmed by the ratio of the slopes of the linear parts of the experimental curve to the left and right from the point of kink. The departure from the linearity near the sample's zero position is determined by the simultaneous falling of the forward and specularly reflected beams to the entrance slit.

By measuring the ratio

$$G = |I_0(\theta') - I_0(\theta'')|/|l(\theta' - \theta'')|, \qquad (6)$$

where θ' and θ'' are arbitrary values of the grazing angle in the linear segment of the curve $I_0(\theta)$ and l is the distance between the sample edge and O_1-axis, we determine the number of quanta per unit width of the beam cross section in the zone of the refracting sample edge.

According to [9], the intensity of the refracted beam can be determined from the expression

$$I_{rr}(\theta_1) = G[1 - R(\theta_1)]\theta_1\mu^{-1}, \qquad (7)$$

where $R(\theta_1)$ is the experimentally measured or calculated coefficient of specular reflection, μ is the linear attenuation coefficient for the radiation.

Figure 5 shows the intensities of the refracted radiation for Si and GaAs samples obtained experimentally and calculated with formula (7). Taking into account instrumental errors and the imperfection of the side face surface, which is obtained by splitting the initial disks of Si and GaAs single crystals, the agreement between these data is satisfactory. Thus, the above estimates of the effective cross section of the refracted beam are confirmed.

The angular parameters of the refracted radiation were determined for fixed grazing angles θ_1 by scanning the rotating support, which holds the detecting system with the 30-μm-wide entrance slit (Fig. 3). Figure 6 shows the measured intensity diagrams for the CuK_α of a GaAs sample as a function of the angle of scattering ψ measured from the direction of the primary beam axis. No refraction occurs at $\theta_1 < \theta_c = 0.309°$ (curve *1*), and only peaks of the primary and specularly reflected beams are observed. In the angular interval between these beams, the radiation emerging through the side face has an angular distribution without a pronounced maximum. This agrees with the known description of the energy flux trajectory at the total external reflection (total internal reflection in optics) [2]. At a comparatively small (0.02°) excess of the critical angle, a reflected radiation peak additionally arises (curve *2*), which, as it follows from Eq. (5), is narrowed with further increase in θ_1 (curve *3*).

For convenience in evaluating the angular width, Fig. 7 shows several refractograms for GaAs in a linear scale. We must pay attention to the following important result. The full-widths $\Delta\varphi_e$ measured at half-maximum (FWHM) of the refraction peaks at grazing angles θ_1 of 0.372° ($1.2\theta_c$) and 0.403° ($1.3\theta_c$) are 0.041° and 0.034°, respectively. For these angles θ_1, the effective

width of the refracted beam at the exit from the side face, which is defined as the value numerically equal to z_e (i.e., at a level of the intensity drop by a factor e), must be 93.6 and 117 nm. Then, in accordance with the theory of prism spectrometers [1, 10, 11], in which the Fraunhofer diffraction is actually considered, the calculated angular FWHM $\Delta\varphi_c$ of the refracted beam of the CuK_α line must be 0.094° (1.65 mrad) and 0.075° (1.31 mrad).

The $\Delta\varphi_e$ values measured experimentally exceed true ones as a result of blurring of the spread function of the slit, divergence of the primary beam, and its angular broadening in refraction ($C_a < 1$, see Eq. (4)). Assuming that all these dependences are described by Gaussian functions, we obtain the following estimates of the true angular broadening: $\Delta\varphi_{e0} = 0.038°$ at $\theta_1 = 1.2\theta_c$ and $\Delta\varphi_{e0} = 0.031°$ at $\theta_1 = 1.3\theta_c$. Thus, the experimental $\Delta\varphi_{e0}$ values are much smaller than calculated ones, and the difference observed is substantially higher than the experimental error.

According to the theory of prism spectrometers, the spectral resolution $A = \lambda/\Delta\lambda$ is associated with the diffraction limit. In the case when the refracted beam is parallel to the base of a prism, we have

$$\lambda/\Delta\lambda \cong bdn/d\lambda, \quad (8)$$

where b is the size of the base of the entirely illuminated prism. Taking into consideration that, in our case, refraction occurs only at a single boundary, and expressing b in terms of z_e, we derive

$$\lambda/\Delta\lambda \cong z_e dn/(2\theta_c d\lambda). \quad (9)$$

Choosing a pair of lines with wavelengths of 0.154 and 0.139 nm and substituting the corresponding parameters into formula (9), we obtain $A \approx 3$ for GaAs and ~3.5 for Si. This means that, from the formal viewpoint, the selected lines must not be resolved. Figure 8 shows experimental refractograms for the GaAs sample at the CuK_α and CuK_β lines at grazing angles of $1.1\theta_c$ and $1.3\theta_c$. The signal intensity of the CuK_β line is rescaled by multiplying by the intensity ratio at the maxima. The comparison shows that the dispersive properties of the sample used ensure spatial separation of the CuK_α and CuK_β characteristic lines. This confirms an earlier conclusion that the actual angular divergence of the refracted beam is appreciably smaller than that formally evaluated from the diffraction limit.

In order to evaluate the angular parameters of the refracted radiation more accurately, it is expedient to increase the distance from the sample to the detecting device and to utilize a two-coordinate detector. Figure 9 presents two-dimensional images of the intensity distribution of the X-ray flux in the plane perpendicular to the direct beam at a distance of 570 mm from the O_1-axis for the refraction of a polychromatic beam at edges of Si, diamond, and GaAs plates. The images are read out from a photographic film by a video camera. The edge bands are traces of intersection of the image plane with the direct (D) and specularly reflected (Rl) beams. The refracted radiation (Rr) of the characteristic lines forms a pair of bands positioned close to each other near the direct beam trace. The values of z_e for the CuK_α line and, respectively, the effective widths of the beams $h = z_e$ near the side faces of the Si, GaAs, and diamond refractors are 81 nm, 96 nm, and 1.8 μm.

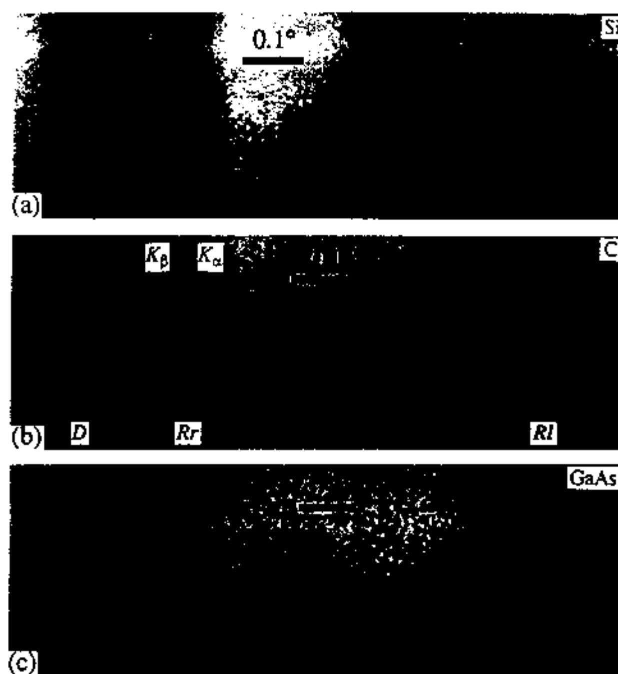

Fig. 9. Images of the forward (D), refracted (Rr), and specularly reflected (Rl) beams in the zy-plane, which is perpendicular to the forward beam, at a distance of 570 mm from the O_1-axis: (a) Si single crystal, $\theta_1 = 0.23°$; (b) diamond, $\theta_1 = 0.327°$; and (c) GaAs single crystal, $\theta_1 = 0.374°$.

The observed positions of the peaks of the refracted radiation satisfactorily coincides with those calculated from the tabulated data [12–14]. The angular widths of the refracted beams for the CuK_α and CuK_β lines with an effective cross section of ~100 nm are much smaller than the diffraction limit $\Delta\varphi$, which is calculated by using the theory of optical spectrometers [1, 10, 11], thus ensuring the resolution of the characteristic lines. This is confirmed by the above data of refractogram measurements with narrow-slit scanning. A detailed analysis of all factors that determine this result is beyond the framework of this study. We only mention that, in contrast to the Fraunhofer diffraction, in this case, the distributions of the intensity I and the amplitude of the electric vector $\mathbf{E}$ along the refracted-wave front do not coincide. In the z-axis direction, $|\mathbf{E}|$ falls in the sample material according to the law $\exp(-2\pi\beta_2 z/\lambda\theta_2)$, and $I = |\mathbf{E}|^2$ changes as $\exp(-4\pi\beta_2 z/\lambda\theta_2)$. Since the angular distribution of the intensity in the far zone depends on the more slowly changing distribution $\mathbf{E}(z)$, the angular width of the beam must be much smaller than the diffraction limit evaluated as $\Delta\varphi = \lambda/h$ at $h = z_e$.

CONCLUSION

One of the most interesting fields of application of the proposed method is the layer-by-layer probing of thin-film structures through the side face. Structural investigations of single-crystal films can be performed by passing a fraction of the primary radiation over the refractor surface, because the angular departure of the refracted beam from the forward one may reach 0.2°–0.4° for a wavelength of 1.5–2 Å. As a rule, this is appreciably larger than the diffraction half-width of structural reflections. In order to analyze the composition of films by their X-ray fluorescence spectra, the forward radiation should be suppressed with an absorbing shield located near the exit face of the refractor. An important advantage of the refraction technique is the possibility of controlling the cross section and angular divergence of the probing beam.

The results obtained in this study show that ribbon beams with a cross section of 300–500 μm^2, an effective thickness of ~0.1 μm, and an intensity of $>10^4$ quanta/s at the fundamental characteristic spectral line can be obtained by using ordinary X-ray tubes with stationary anodes. Needlelike beams can be obtained with synchrotron radiation sources.

ACKNOWLEDGMENTS

We are grateful to I.P. Kazakov and R.A. Khmel'nitskii for the samples.

REFERENCES

1. Landsberg, G.S., *Optika* (Optics), Moscow: Nauka, 1976.
2. Kaliteevskii, N.I., *Volnovaya optika* (Wave Optics), Moscow: Nauka, 1971.
3. Lagomarsino, S., Jark, W., Fonzo, S.Di., *et al.*, *J. Appl. Phys.*, 1996, vol. 49, no. 8, part 1, p. 4471.
4. Blokhin, M.A., *Fizika rentgenovskikh luchei* (X-ray Physics), Moscow: Gos. Izd. Tekh. Teor. Lit., 1957.
5. Gao, N., Ponomarev, I.Yu., Xiao, Q.F., *et al.*, *Appl. Phys. Lett.*, 1997, vol. 71, no. 23, p. 3441.
6. Nikulin, A.Yu. and Davis, J.R., *Opt. Commun.*, 1998, vol. 155, nos. 4–6, p. 231.
7. Ioneda, I., *Phys. Rev.*, 1963, vol. 131, p. 2010.
8. Touryanskii, A.G., Vinogradov, A.V., and Pirshin, I.V., *Prib. Tekh. Eksp.*, 1999, no. 1, p. 105.
9. Touryanskii, A.G. and Pirshin, I.V., *Prib. Tekh. Eksp.*, 1999, no. 6, p. 104.
10. Zaidel', A.N., Ostrovskaya, G.V., and Ostrovskii, Yu.I., *Tekhnika i praktika spektroskopii* (Techniques and Practice of Spectroscopy), Moscow: Nauka, 1976.
11. Tarasov, K.I., Blokh, A.A., Golyandin, N.S., and Kossova, N.F., *Proektirovanie spektral'noi apparatury* (Design of Spectral Instruments), Leningrad: Mashinostroenie, 1980.
12. Blokhin, M.A. and Shveitser, I.G., *Rentgenospektral'nyi spravochnik* (Handbook for X-ray Spectra), Moscow: Nauka, 1982.
13. Henke, B.L., Gullikson, E.M., and Davis, J.C., *X-ray Interactions: Photoabsorption, Scattering, Transmission, and Reflection at E = 50–30000 eV, Z = 1–92. Atomic Data and Nuclear Data Tables*, 1993, vol. 54, no. 2, pp. 181–342.
14. *Fizicheskie velichiny. Spravochnik* (Physical Quantities. Handbook), Grigor'ev, I.S. and Meilikhov, E.Z., Eds., Moscow: Energoatomizdat, 1991.